Residual Vision in a Scotoma: Implications for Blindsight

Robert Fendrich,* C. Mark Wessinger, Michael S. Gazzaniga

Blindsight, the ability of some blind patients to describe attributes of stimuli they have no conscious awareness of seeing, has been attributed to a secondary (retinotectal) visual pathway. However, it has also been proposed that blindsight could be due to residual function within the primary (geniculostriate) visual pathway. Data have now been obtained that support the second alternative. With an image stabilizer ensuring the accurate retinal placement of stimuli, dense visual field mapping was carried out with a hemianopic patient. This perimetry revealed, embedded in the patient's scotoma, an isolated 1-degree island of residual vision that was not disclosed by conventional perimetric methods. Stimuli presented to this island could be detected and discriminated, although the subject reported he did not see them. The existence of this island of vision implies a corresponding island of functioning cortex within the patient's lesion. Other instances of blindsight may be mediated by similar islands of functioning cortex.

Blindsight refers to residual visual capacities in the absence of acknowledged awareness (*1, 2*). In humans, the major (geniculostriate) visual pathway projects from the retina to primary (striate) visual cortex by way of the lateral geniculate nucleus. Some patients rendered blind by striate lesions have demonstrated an ability to detect and localize stimuli that they do not report seeing (*1, 3, 4*). Patients have also demonstrated an ability to discriminate the orientation (5), motion (6), and wavelength (*7*) of such stimuli. Blindsight has been attributed to a secondary (retinotectal) visual pathway (*2, 8, 9*), which projects from the retina to higher (extrastriate) cortical regions through the superior colliculus. Some animal research supports this hypothesis (*10*). Alternatively, blindsight may be mediated by surviving vestiges of geniculostriate function (*3, 11*) or direct projections from the lateral geniculate nucleus to extrastriate cortex (*12*). We present evidence from a hemianopic patient that supports these alternative possibilities.

Patient CLT, tested with informed consent, is a 54-year-old male who had a right posterior cerebral artery stroke in 1987. This stroke produced a dense left homonymous hemianopia, with some sparing in the central portion of the lower left visual quadrant (quadrant macular sparing). Figure 1 shows visual fields obtained with computerized mapping (perimetry). Figure 2 shows T1 and T2 weighted magnetic resonance images, which reveal a large lesion within CLT's right occipital cortex.

With conventional computerized perimetry, test stimuli are spaced about 6° apart. Closer spacing is possible, but the normal instability of the eye during fixation (which may be exacerbated in patients with visual impairments) limits the accuracy with which stimuli can be positioned on the retina. We eliminated this problem by using a Purkinje image eyetracker (with 1 arc min of resolution) (*13*) coupled to an image stabilizer (*14*). CLT viewed stimuli with his right eye by means of mirrors controlled by the eyetracker outputs. If CLT's gaze shifted, the mirrors shifted the visual scene with the eye, holding the retinal position of stimuli constant (*15*). Consequently, specific positions on our display screen stimulated consistent retinal locations, irrespective of the patient's eye motions. This permitted extended stimulus presentations.

To maximize sensitivity and eliminate criterion effects, we used interval two alternative forced choice methodology (*16*). For each trial, tones delimited two consecutive 0.6-s intervals. During one of these intervals, a black circle 1° in diameter (<1 cd/m^2) flashed three times for 96 ms on a white background (10 cd/m^2 through the stabilizer's viewing optics) at a randomly selected test location. CLT was required to decide which interval contained the target presentation. Confidence ratings were taken on 70% of the trials (1 = low, 5 = high). Stimuli were displayed on a Macintosh II monitor. Sixty-eight locations in the central 15° by 24° of CLT's left visual field and eight locations in his right visual field were tested. Left-field test locations were separated horizontally (center to center) by 2.5° and vertically by 2°, beginning 1° from the horizontal meridian and 1.5° from the vertical meridian. Data were obtained over 30 test sessions. Overall, there were 36 to 292 presentations at each test location.

Targets in the right visual field were detected with an accuracy exceeding 95%. Stabilized perimetry revealed several features in the left visual field not shown by conventional perimetry (Fig. 3). A band of residual vision extends downward along the vertical meridian in the lower left quadrant. In the upper left quadrant, a band of vision extends out to 7° along the horizontal meridian. At 7° above the horizontal meridian, a peninsula of vision extends leftward from the vertical meridian. Most important, there is an isolated island of vision 7° above the horizontal meridian and 11.5° left of the vertical meridian. CLT's 65% correct detection at this location is significant ($Z = 3.08$, $n = 166$, $P < 0.00005$) and remains significant with a Bonferroni correction for 68 test locations ($P < 0.01$) (*17*). Surrounding test points gave no indication of residual function. This continued to be the case when we increased the

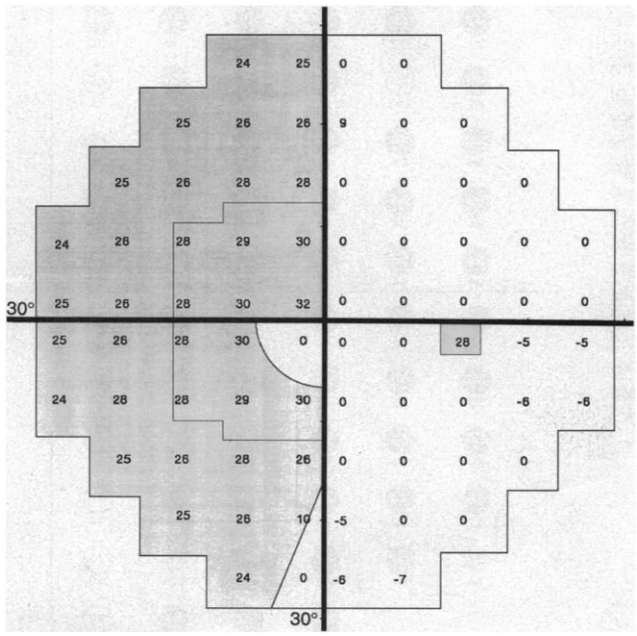

Fig. 1. Standard right-eye perimetry of CLT's visual fields. Data are expressed as decibels below age-corrected normal performance. Shaded portions are the regions diagnosed clinically blind. The inner border in the left visual field surrounds the area we tested; this area includes 12 test points.

Center for Neuroscience, University of California, Davis, CA 95616.

*To whom correspondence should be addressed.

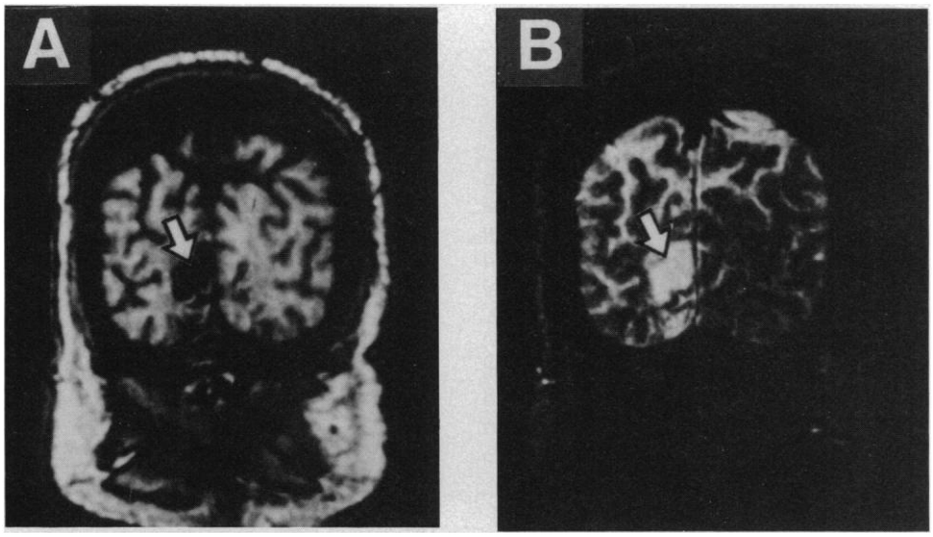

Fig. 2. Coronal magnetic resonance images through CLT's occipital lobe (with the left hemisphere imaged on the right). On the T1 weighted image (**A**) damaged areas appear black or gray. On the T2 weighted image (**B**), which highlights the water content characteristic of damaged tissue, these areas appear white.

diameter of the perimetric target to 2° for a subset of these points. CLT reported that targets were never actually visible in the upper left portion of the screen, and his mean confidence rating of 1.05 for the island of function is comparable to his mean rating of 1.03 for the surrounding blind regions. When queried, CLT insisted that he "never saw anything" in the upper left portion of the visual field, although he occasionally had a sense that "something happened there" (*18*). His detection ability in the island of preserved function therefore has the character of blindsight.

To determine the boundaries of the island of preserved function, we performed denser perimetric mapping, using a 3.66° square matrix of nine stimuli 1° in diameter (Fig. 4). Only at the central test location was detection significantly greater than chance, suggesting that the island of sparing is primarily confined to an area not much larger than 1°. However, some residual function may be present below and to the lower left of the center position.

When we assessed CLT's ability to use information presented to the island of preserved detection, we found that he could not identify the location of stimuli presented within this area. He was unable to report whether an arrow in his seeing field was vertically aligned with a target in his blind field, even when that target was presented in the island of sparing. He was also unable to direct a saccade toward a 1° stimulus flashed at this location. Nevertheless, he could discriminate between a diamond and a square (both 1° on a side) centered within the island of sparing. His accuracy was 65% in this task ($Z = 5.00$, $n = 288$, $P < 0.0001$), which is comparable to his detection performance. His mean confidence rating of 1.06 indicated no conscious awareness of which figure had been displayed. However, when we increased the size of the diamond and square to 2° on a side, CLT's accuracy did not differ from chance (47% correct, $n = 72$). This suggests that CLT's discrimination of the stimuli required a contour edge within the island of sparing. Large stimuli completely blanketed the island, eliminating this contour information.

We also investigated residual visual abilities at two additional locations in CLT's blind field. Both locations were 6.5° left of the vertical meridian; one was 1° above the horizontal meridian and the other 1° below that meridian. At these locations, CLT's confidence ratings and detection accuracies were higher than in the island of sparing (>2 and >90%, respectively). CLT was able to localize and direct a saccade toward stimuli presented to these locations. At the lower field location he could discriminate between a 1° diamond and square (93% correct, $n = 180$),

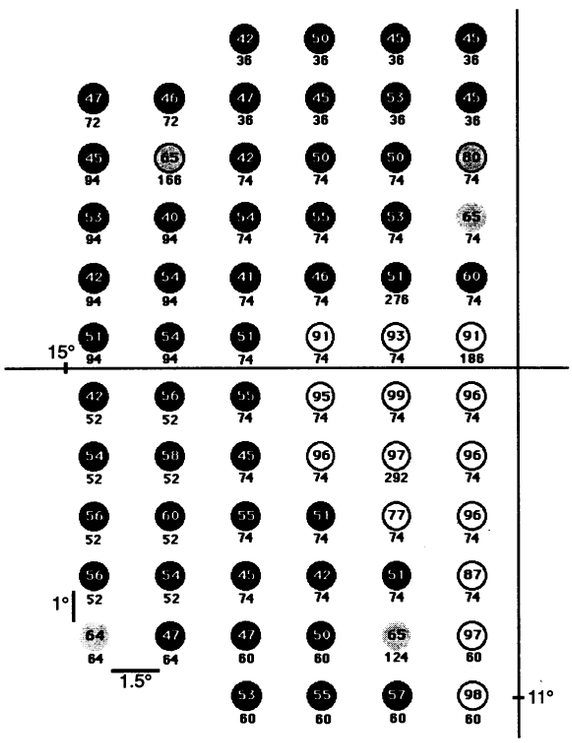

Fig. 3. Results of stabilized image perimetry in CLT's left visual field. The area is 15° horizontal by 24° vertical and contains 68 test locations. Each location is represented by a circle. The number in the circle shows the percentage of correct detections; the number below the circle is the number of trials for that location. White circles show test locations where detection was largely unimpaired. Gray circles with black borders are locations where detection was impaired but significantly better than chance with a Bonferroni correction. Gray circles with no border show locations where detection was better than chance but not with a Bonferroni correction.

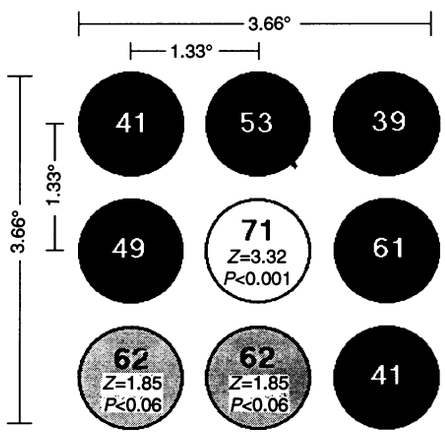

Fig. 4. Detailed stabilized perimetry of the retinal area containing CLT's island of preserved visual function. Large numbers show percentages of correct detection. There were 66 trials at each location. At the center position, performance was significantly above chance and remained so with a Bonferroni correction for nine tests ($P < 0.01$). At the positions shown in gray, accuracy rates were elevated but did not reach significance.

but at the upper field location he could not (50% correct, $n = 180$). However, when the size of the stimulus was increased to 2° on a side, discrimination became possible at both locations. This reveals a pattern of visual abilities that contrasts sharply with that found at the island of sparing.

Because CLT's preserved visual function is limited to an isolated region embedded in his scotoma, it cannot be attributed to a general retinotectal system. The preserved function could be attributed to either a corresponding island of partially preserved striate cortex or an isolated region of partially functioning extrastriate cortex accessed by geniculo-extrastriate projections. Both explanations are viable, but we regard the former as more likely, because a magnetic resonance–based flat-map reconstruction (*19*) of CLT's right hemisphere shows considerable sparing of extrastriate areas but only a minimal region of remaining striate tissue (Fig. 2).

The existence of a small island of sparing embedded within the blind field raises the possibility that similar islands could mediate blindsight in other patients. Visual field mapping that we conducted with one additional patient is commensurate with this possibility. The mapping indicates that regions shown by standard perimetry to have uniformly degraded vision can, with stabilized perimetry, resolve into a mosaic of blind and seeing regions. Patchy distributions of residual vision within scotomas may therefore be more common than previously realized. Of course, the fact that cortical sparing is capable of mediating blindsight does not exclude the possibility that a retinotectal pathway mediates blindsight in some cases. Visual capacities have been reported in the blind field of some hemispherectomy patients (*8, 20*), although these capacities could be attributed to adaptive cortical rearrangements. The evaluation of the role of cortical sparing in blindsight will require detailed visual-field mapping with additional patients. However, our results underscore the fact that manifestations of blindsight must be interpreted with considerable caution. Only when one can rule out the possibility that preserved visual functions are a consequence of preserved cortex can an interpretation based on a retinotectal system be regarded with confidence. Our findings indicate that small regions of preserved visual cortex may be difficult or impossible to detect with conventional perimetric methods.

REFERENCES AND NOTES

1. L. Weiskrantz, E. K. Warrington, M. D. Sanders, J. Marshall, *Brain* **97**, 709 (1974).
2. L. Weiskrantz, *Proc. R. Soc. London Ser. B* **239**, 247 (1990).
3. E. Pöppel, R. Held, D. Frost, *Nature* **243**, 295 (1973).
4. J. Zihl and D. Von Cramon, *Behav. Brain Res.* **1**, 287 (1980).
5. L. Weiskrantz, *Brain* **110**, 77 (1987).
6. J. L. Barbur *et al.*, *ibid.* **103**, 905 (1980).
7. P. Stoerig, *ibid.* **110**, 869 (1987); _____ and A. Cowey, *Nature* **342**, 916 (1989).
8. M. T. Perenin and M. Jeannerod, *Neuropsychologia* **16**, 1 (1978).
9. R. Rafal, J. Smith, J. Krantz, A. Cohen, C Brennan, *Science* **250**, 118 (1990).
10. C. W. Mohler and R. H. Wurtz, *J. Neurophysiol.* **40**, 74 (1977); P. Pasik and T. Pasik, in *Contributions to Sensory Physiology*, W. D. Neff, Ed. (Academic Press, New York, 1982), vol. 7, pp. 147–200; C. G. Gross, *Neuropsychologia* **29**, 497 (1991).
11. J. Campion, R. Latto, Y. M. Smith, *Behav. Brain Sci.* **6**, 423 (1983).
12. A. Cowey and P. Stoerig, *Trends Neurosci.* **14**, 140 (1991).
13. H. D. Crane and C. M. Steele, *Appl. Opt.* **17**, 691 (1978).
14. H. D. Crane and M. R. Clark, *ibid.*, p. 706.
15. To calibrate stabilization, we used a beam splitter to superimpose the image of a nonstabilized screen on the image of the stabilized screen. A matrix of five fixation points and a 1° outline square were presented on the nonstabilized screen. The position of the square was determined by the eyetracker outputs, which were adjusted so that this square surrounded each fixation point as the subject looked at that point. Finally, the stabilizer gains and offsets were adjusted so a 1° circle on the stabilized screen appeared to superimpose exactly on the square and remained superimposed when the subject moved his eyes. This calibration was checked periodically during each testing session.
16. N. A. Macmillan and C. D. Creelman, *Detection Theory* (Cambridge Univ. Press, Cambridge, 1991), pp. 117–140.
17. A second potential island of preserved function with 64% correct detection ($Z = 2.12$, $n = 64$, $P < 0.02$) occurs at the lower left edge of the field but does not reach significance with a Bonferroni correction.
18. CLT was conservative in his confidence criteria, when he "had a sense" of some event but did not believe he had actually seen anything, he regarded his choice as a guess and reported "1."
19. M. L. Jouandet *et al.*, *J. Cognitive Neurosci.* **1**, 88 (1989).
20. A. Ptito *et al.*, *Brain* **114**, 497 (1991).

21. We thank CLT for his commitment to our extended testing program, supported by NIH/National Institute of Neurological Diseases and Stroke grant P01 NS17778-10 and the James S McDonnell Foundation.

18 May 1992; accepted 7 October 1992

Amelioration of Autoimmune Encephalomyelitis by Myelin Basic Protein Synthetic Peptide–Induced Anergy

Amitabh Gaur, Brook Wiers, Angela Liu, Jonathan Rothbard, C. Garrison Fathman*

Experimental autoimmune encephalomyelitis (EAE), a demyelinating disease of the central nervous system that can be induced in susceptible strains of mice by immunization with myelin basic protein (MBP) or its immunodominant T cell determinants, serves as a model of human multiple sclerosis. Tolerance to MBP in adult mice was induced by intraperitoneal injection of synthetic peptides of immunodominant determinants of MBP and prevented MBP-induced EAE. Furthermore, tolerance-inducing regimens of peptides administered to mice after the disease had begun (10 days after induction with MBP) blocked the progression and decreased the severity of EAE. Peptide-induced tolerance resulted from the induction of anergy in proliferative, antigen-specific T cells.

Over the past decade, it has become apparent that synthetic peptides corresponding to the major immunodominant T cell determinants of native protein antigens can induce unresponsiveness both to themselves and to the native protein antigen in neonatal and adult mice (*1–4*). The use of peptide-specific tolerance as a means to treat human autoimmune disease is a consequence of these studies. Murine EAE is a model of human multiple sclerosis (MS) (*5*) and is caused by an immune response to MBP. We have now induced tolerance to synthetic peptides corresponding to the major immunodominant determinants of MBP (peptides Ac 1–11 and 35–47) or to intact MBP by intraperitoneal injection of an emulsion of the peptide or protein in incomplete Freund's adjuvant (IFA), as has been described for tolerance induction to other proteins or peptides (*3*). Two weeks after administration of tolerogen, mice were injected subcutaneously at the base of the tail with the same peptide antigen or the intact protein emulsified in complete Freund's adjuvant (CFA), the usual route of immunization. T cell proliferative assays performed on regional draining lymph node cells 10 days later revealed that the mice had been made tolerant to the peptide or protein administered as tolerogen. Both peptides Ac 1–11 and 35–47 induced tolerance to recall challenge by themselves in PL/J mice (Fig. 1A) (*6*).

In a separate experiment, PL/J mice were injected intraperitoneally with Ac

A. Gaur, B. Wiers, C. G. Fathman, Stanford University School of Medicine, Division of Immunology and Rheumatology, Stanford, CA 94305.
A. Liu and J. Rothbard, ImmuLogic Pharmaceutical Corporation, Palo Alto, CA 94304.

*To whom correspondence should be addressed.